Advances in Difference Equations
a SpringerOpen Journal

RESEARCH Open Access

A simple mathematical model for Guillain–Barré syndrome

Mohammed Fathy Elettreby[1,2*], Elsayed Ahmed[2] and Muntaser Safan[2,3]

*Correspondence:
mohfathy@mans.edu.eg
[1]Mathematics Department, Faculty of Science, King Khalid University, Abha, Saudi Arabia
[2]Mathematics Department, Faculty of Science, Mansoura University, Mansoura, Egypt
Full list of author information is available at the end of the article

Abstract

In this paper, four different forms of a model to describe the dynamics of autoimmune diseases (with emphasis on Guillain–Barré syndrome) are proposed. In the first two cases, the immune response is supposed to be linear, while in the other two cases it is supposed to be in the Holling type III form. In case of linear immune response, the model has a basic reproduction number and shows forward bifurcation. However, in the nonlinear Holling type III immune response cases, the model does not have a basic reproduction number and two positive equilibria do exist for a range of the parameters. The stability analysis of the model's steady states has been established. Our analytical results have been illustrated by numerical simulations.

MSC: 92Bxx; 37Fxx; 34Cxx

Keywords: Guillain–Barré syndrome; Steady states; Stability analysis; Tolerance; Flare-up; Dormancy

1 Introduction

Understanding the way the immune system works and how autoimmune diseases occur is a very complex process. However, the main task of the immune system is to prevent self-reactive cells from attacking self organ by some kind of apoptosis processes [1]. Autoimmune diseases are a group of diseases of disturbance of the immune system like rheumatoid arthritis system lupus, insulin-dependent diabetes mellitus type-I (IDDM), multiple sclerosis (MS), and others. An autoimmune disease occurs when any organ or tissue in the body becomes a target for the immune system attacks [1, 2]. The cases of autoimmune diseases can be characterized by tolerance, flare-ups, or dormancy. The principal defendant in these cases is the T-cells. Also, virus infection is associated with the exacerbation of the autoimmune diseases [3].

Guillain–Barré syndrome (GBS) is a scarce autoimmune disease in which the peripheral nerves are attacked by the person's immune system [4]. This attack can affect the nerves that control the muscle movement, as well as the nerves that transmit the pain, the temperature, and the touch sensations [5]. Also, this attack can lead to loss of sensation in arms and/or legs and muscle weakness. This syndrome can affect people of all ages, but it is more popular in adult males [6]. Approximately one person in every 100,000 is affected. Most patients of this disease fully recover from even the most severe cases. Typically, symptoms continue for a few weeks, where most cases recover without acute and

long-term neurological complications. The first symptoms of GBS include tingling sensations or at least weakness. Usually, these symptoms begin in the legs and can spread to other organs like the arms and face. Severe cases of GBS are rare, but for those individuals, these symptoms can lead to paralysis of the legs, the arms, or the muscles in the face. In 20–30% of patients, it is hard to breathe because the chest muscles are affected. Also, the ability to speak or even swallow may become affected in the severe cases of GBS. The life of these cases is threatened, and affected patients should be treated in intensive care units [7]. The treatment of this disease may include some immunological therapies and supportive care. Even in the best of settings, 3–5% of GBS patients die from complications which can include blood infection, paralysis of the muscles that control breathing, cardiac arrest, or lung clots [8–10].

Frequently, GBS is preceded by infection. This infection can be viral or bacterial. Also, GBS may occur due to surgery or vaccine administration. As in the case of Zika virus infection, a sudden increase in the number of patients of GBS has been observed in the affected countries. Zika virus infection is a trigger of GBS, this is the most likely explanation from the outbreaks of Zika virus infection and the GBS [11, 12]. The association of GBS with Zika and other flavivirus has been reviewed in Uncini et al. [13]. Recently, the transmission dynamics of Zika virus infection has been extensively studied [14–19] based on models on the population level. For example, Bonyah and Okosun [15] studied the optimal control strategy to minimize the spread of Zika virus disease. The authors showed that a strategy based on prevention, treatment of infected humans, and use of insecticide to kill mosquitoes would be the best way to reduce the spread of Zika. Another research [17] aimed to identify the recovery time and predict the endemic condition of Zika virus. Moya [18] introduced and studied a mathematical model for the transmission of Zika virus disease on the population level where two time delays (one delay for the beginning of human symptoms and the other is the time taken by the mosquito to develop the pathogen) have been considered. Charles et al. [19] developed and analyzed a spatiotemporal model to describe the transmission dynamics of Zika virus disease and deduced potential control strategies. In addition to the equilibrium and stability analyses, the authors showed the existence of traveling wave solutions that propagate with the speed of disease spread. However, the dynamics GBS (which is a complication of Zika) is poorly studied. In this work, four different forms of a model describing the dynamics of autoimmune diseases with emphasis on Guillain–Barré syndrome are introduced.

To the best of our knowledge, this is the first research that attempts to model Guillain–Barré syndrome. In Sect. 2, we model the mechanism of Guillain–Barré syndrome by proposing a simple model as a system of two ordinary differential equations. In Sect. 3, we propose a linear immune response and investigate the model with two cases of the growth function of the target cell population. In Sect. 4, we propose a nonlinear immune response with the same two cases of the growth function of the target cell population. Finally, we summarize and conclude our results in Sect. 5.

2 The model

There are several medical literature sources on autoimmune diseases but there are few mathematical literature papers. Here, we present the first paper that represents the Guillain–Barré syndrome as a simple mathematical model. Consider $x(t)$ to be the population size of the target cells (healthy cells) at time t which determine the symptoms of

autoimmune disease patients. Therefore, if it is large, then the symptoms are mild; otherwise, the symptoms are severe. Let $y(t)$ be the population size of the immune cells inducement at time t. The growth function of the target cell population $G_1(x(t))$ and the personal immune response function $G_2(x(t), y(t))$ play the basic role in our model. Then the dynamics of the target cells and the immune cells give us the following basic model of the Guillain–Barré syndrome:

$$\begin{aligned} \frac{dx(t)}{dt} &= G_1\big(x(t)\big) - \beta x(t)y(t), \\ \frac{dy(t)}{dt} &= G_2\big(x(t), y(t)\big) - \gamma y(t), \end{aligned} \tag{1}$$

where the term $\beta x(t)y(t)$ represents the damage that occurred in the target cells due to their interaction with the immune system and the parameter γ is the death rate of the immune cells.

3 Linear immune response function

3.1 Linear target cell growth function

Firstly, we propose that the evolution of the target cells population, in the simplest form, is a linear function of $x(t)$. Then model (1) reads as follows:

$$\begin{aligned} \frac{dx(t)}{dt} &= F_1\big(x(t), y(t)\big) = \lambda - \mu x(t) - \beta x(t)y(t), \\ \frac{dy(t)}{dt} &= F_2\big(x(t), y(t)\big) = kx(t)y(t) - \gamma y(t), \end{aligned} \tag{2}$$

where λ is the rate of producing new cells of the target cells from the bone marrow, μ is the natural death rate of the target cells, β is the rate at which the immune cells find and attack the target cells [20, 21], and k is the average magnitude of activation of the immune response per unit time.

Model (2) is nonlinear and has no time-dependent explicit solution. Therefore, we study the model at the long time run. Equating the derivatives of (2) by zero and solving the resulting nonlinear algebraic system with respect to the equilibrium state variables $\bar{x}$, $\bar{y}$, we get the two equilibria

$$E_{1,0} = \left(\frac{\lambda}{\mu}, 0\right)' \quad \text{and} \quad E_{1,1} = (\bar{x_1}, \bar{y_1})' = \left(\frac{\gamma}{k}, \frac{k\lambda - \mu\gamma}{\beta\gamma}\right)' = \left(\frac{\gamma}{k}, \frac{\mu}{\beta}(R_{0,1} - 1)\right)', \tag{3}$$

where the $'$ means vector transpose. The endemic equilibrium $E_{1,1}$ does exist if and only if the basic reproduction number $R_{0,1} > 1$, where

$$R_{0,1} = \frac{k\lambda}{\gamma\mu}. \tag{4}$$

The local stability analysis of these equilibria is established by studying the Jacobian matrix of (2) at these equilibria. The Jacobian matrix evaluated at the trivial equilibrium $E_{1,0}$ is

$$J_{1,0} = \begin{pmatrix} -\mu & -\frac{\beta\lambda}{\mu} \\ 0 & \frac{k\lambda}{\mu} - \gamma \end{pmatrix}.$$

It has the eigenvalues $-\mu$ and $\frac{k\lambda}{\mu} - \gamma$. Hence, the trivial (boundary) equilibrium $E_{1,0}$ is locally asymptotically stable if and only if $R_{0,1} < 1$.

Similarly, the Jacobian matrix computed at the endemic (interior) equilibrium $E_{1,1}$ is

$$J_{1,1} = \begin{pmatrix} -\frac{k\lambda}{\gamma} & -\frac{\beta\gamma}{k} \\ k\frac{k\lambda-\mu\gamma}{\beta\gamma} & 0 \end{pmatrix}.$$

Its trace is $\operatorname{tr}(J_{1,1}) = -k\lambda/\gamma < 0$, while its determinant is $\det(J_{1,1}) = k\lambda - \mu\gamma > 0$ if and only if $R_{0,1} > 1$. Hence, $E_{1,1}$ is locally asymptotically stable iff $R_{0,1} > 1$. We summarize the above results in the following proposition.

Proposition 1 *The linear target cell growth function's model* (2) *has a boundary equilibrium $E_{1,0}$ which is locally asymptotically stable if and only if the basic reproduction number $R_{0,1} < 1$. Moreover, it has an interior equilibrium $E_{1,1}$ that exists if and only if $R_{0,1} > 1$. This interior equilibrium $E_{1,0}$ is locally asymptotically stable whenever it exists.*

Global stability analysis could be done with an approach based on the use of Liapunov functions. For the trivial (boundary) equilibrium, we consider the following Liapunov function:

$$V_{1,0} = k\left(x - \frac{\lambda}{\mu} - \frac{\lambda}{\mu}\ln\frac{\mu x}{\lambda}\right) + \beta y. \tag{5}$$

Its time derivative is

$$\begin{aligned}\dot{V}_{1,0} &= k\dot{x}\left(1 - \frac{\lambda}{\mu x}\right) + \beta\dot{y} = k\left(1 - \frac{\lambda}{\mu x}\right)(\lambda - \mu x - \beta xy) + \beta(kxy - \gamma y) \\ &= \lambda k\left(1 - \frac{\lambda}{\mu x}\right)\left(1 - \frac{\mu x}{\lambda}\right) - \gamma\beta y\left(1 - \frac{k\lambda}{\mu\gamma}\right) \\ &= -\lambda k\left(\sqrt{\frac{\lambda}{\mu x}} - \sqrt{\frac{\mu x}{\lambda}}\right)^2 - \gamma\beta y(1 - R_{0,1}).\end{aligned}$$

Hence, $\dot{V}_{1,0} < 0$ if $R_{0,1} < 1$. Thus, the boundary equilibrium $E_{1,0}$ is globally asymptotically stable iff $R_{0,1} < 1$.

Similarly, the global stability of the endemic equilibrium $E_{1,1}$ for $R_{0,1} > 1$ could be shown by considering the Liapunov function

$$V_{1,1} = k\left(x - \frac{\gamma}{k} - \frac{\gamma}{k}\ln\frac{kx}{\gamma}\right) + \beta\left(y - \bar{y_1} - \bar{y_1}\ln\frac{y}{\bar{y_1}}\right). \tag{6}$$

Its time derivative over trajectories is

$$\begin{aligned}\dot{V}_{1,1} &= k\dot{x}\left(1 - \frac{\gamma}{kx}\right) + \beta\dot{y}\left(1 - \frac{\bar{y_1}}{y}\right) \\ &= \mu\gamma\left(1 - \frac{\gamma}{kx}\right)\left(1 - \frac{kx}{\gamma}\right) + k\beta\left(1 - \frac{\gamma}{kx}\right)\left(\frac{\gamma}{k}\bar{y_1} - xy\right) + \beta(kxy - \gamma y)\left(1 - \frac{\bar{y_1}}{y}\right)\end{aligned}$$

$$= \mu\gamma\left(1-\frac{\gamma}{kx}\right)\left(1-\frac{kx}{\gamma}\right)+\beta\gamma\bar{y_1}\left(2-\frac{\gamma}{kx}-\frac{kx}{\gamma}\right)$$

$$= -\gamma(\mu+\beta\bar{y_1})\left(\sqrt{\frac{\gamma}{kx}}-\sqrt{\frac{kx}{\gamma}}\right)^2 < 0.$$

Hence, the endemic equilibrium $E_{1,1}$ is globally asymptotically stable whenever it exists, and we show the following proposition.

Proposition 2 *The boundary* (*trivial*) *equilibrium* $E_{1,0}$ *for the linear target cell growth function's model* (2) *is globally asymptotically stable if its basic reproduction number* $R_{0,1} < 1$, *while if* $R_{0,1} > 1$, *then the endemic* (*interior*) *equilibrium* $E_{1,1}$ *is globally asymptotically stable*.

It is clear that the stability of the endemic state $E_{1,1}$ cancels the stability of the trivial one $E_{1,0}$. However, if the parameters λ, μ, and γ are kept fixed, then a value of $R_{0,1} > 1$ corresponds to a value of $k > \gamma\mu/\lambda$. Hence, the essential difference between the two cases is the value of the parameter k.

Numerical simulations for model (2) have been carried out, where it is revealed that the solutions do not depend on the initial conditions, see Fig. 1(a), (b), (c). The figure shows a tolerance of the immune response, i.e., the induced immune cells cannot be activated, $y(t)$ vanishes, and the autoimmune disease does not develop. The figure shows further that if k is small, then the damage is small, the immune-induced cells are not activated, and the number of target cells does not decrease. However, if the value of k is large, then the damage is great, the immune-induced cells are activated, and the number of target cells decreases. Therefore, the patient with a higher value of k has a higher probability of developing an autoimmune disease. Moreover, increasing the value of k moves the case of

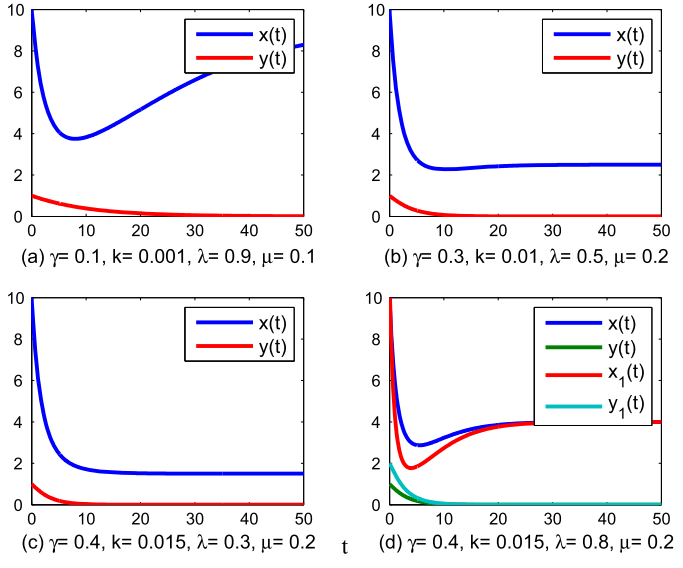

Figure 1 The first three figures show the curves of target cells $x(t)$ and the immune cells induced $y(t)$ at $\beta = 0.5$, $x(0) = 10$, $y(0) = 1$, and different values of the parameters. The fourth one shows that it does not depend on the initial values of $x(t)$, $y(t)$ where we take another initial value $x1(0) = 11$, $y1(0) = 2$

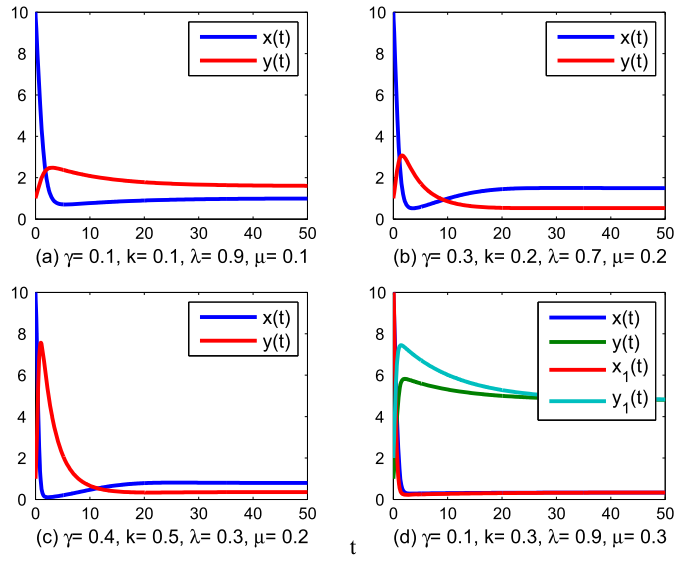

Figure 2 The first three figures show the curves of target cells $x(t)$ and the immune cells induced $y(t)$ at $\beta = 0.5$, $x(0) = 10$, $y(0) = 1$, and different values of the parameters. The fourth one shows that it does not depend on the initial values of $x(t)$, $y(t)$ where we take another initial values $x_1(0) = 11$, $y_1(0) = 2$

the patient from tolerance to acute. After some time, the acute symptoms shift to a chronic case.

Simulations with different values of the above parameters have been done, and they showed that the steady state $E_{1,1}$ is always stable. Figure 2 shows acute and chronic symptoms, which means that the immune-induced cells are activated, $y(t)$ does not vanish, and the patient develops an autoimmune disease.

3.2 Nonlinear target cell growth function

Assume now that the evolution of the target cells population is a nonlinear function of $x(t)$, and it is in logistic form [22, 23]. Hence, model (1) reads as follows:

$$\begin{aligned} \frac{dx(t)}{dt} &= \lambda - \mu x(t) + px(t)\left(1 - \frac{x(t)}{L}\right) - \beta x(t)y(t), \\ \frac{dy(t)}{dt} &= kx(t)y(t) - \gamma y(t), \end{aligned} \tag{7}$$

where p is the maximum proliferation rate of the target cells and L is the target cell population density at which proliferation shuts off. The added term (logistic term) represents the created target cells by the proliferation of the target cells, and the parameter β is as defined above [20, 21, 23].

Again, to find the steady states $(\overline{x}, \overline{y})'$ of system (7), we put

$$\begin{aligned} \left.\frac{dx(t)}{dt}\right|_{(\overline{x},\overline{y})} &= F_1(\overline{x}, \overline{y}) = 0, \\ \left.\frac{dy(t)}{dt}\right|_{(\overline{x},\overline{y})} &= F_2(\overline{x}, \overline{y}) = 0. \end{aligned} \tag{8}$$

On solving the equations of system (8), we get the following steady states:

$$E_{2,0} = (\overline{x}, 0)', \qquad E_{2,1} = \left(\frac{\gamma}{k}, \frac{k\lambda}{\beta\gamma} + \frac{(p-\mu)}{\beta} - \frac{p\gamma}{k\beta L}\right)',$$

where

$$\overline{x} = \frac{L}{2p}\left((p-\mu) + \sqrt{(p-\mu)^2 + 4p\lambda/L}\right).$$

The second steady state $E_{2,1}$ does exist if and only if

$$Lk\left(k\lambda + (p-\mu)\gamma\right) > p\gamma^2. \tag{9}$$

This inequality is equivalent to

$$k > \frac{2p\gamma}{L(p-\mu+\sqrt{(p-\mu)^2 + 4p\lambda/L})}. \tag{10}$$

The local stability of the boundary equilibrium point $E_{2,0} = (\overline{x}, 0)$ is studied by considering its corresponding Jacobian matrix

$$J_{2,0} = \begin{pmatrix} -\sqrt{(p-\mu)^2 + 4p\lambda/L} & -\beta\overline{x} \\ 0 & k\overline{x} - \gamma \end{pmatrix},$$

which has the eigenvalues $\epsilon_1 = -\sqrt{(p-\mu)^2 + 4p\lambda/L} < 0$ and $\epsilon_2 = k\overline{x} - \gamma$. Hence, the boundary equilibrium point $E_{2,0}$ is locally asymptotically stable if and only if $R_{0,2} < 1$, where

$$R_{0,2} = \frac{kL(p-\mu+\sqrt{(p-\mu)^2 + 4p\lambda/L})}{2p\gamma} \tag{11}$$

is the basic reproduction number [24] for model (7). Similarly, the Jacobian matrix of model (7) evaluated at the endemic equilibrium $E_{2,1}$ is

$$J_{2,1} = \begin{pmatrix} -\frac{p\lambda}{kL} - \frac{k\lambda}{\gamma} & -\frac{\beta\gamma}{k} \\ \frac{k^2\lambda}{\beta\gamma} + \frac{k(p-\mu)}{\beta} - \frac{p\gamma}{\beta L} & 0 \end{pmatrix}.$$

It is clear that the trace of $J_{2,1}$ is negative, while its determinant is positive if and only if condition (10) holds (i.e., when $R_{0,2} > 1$). Hence, the interior (endemic) equilibrium is locally asymptotically stable whenever it exists. The above results are summarized in the following proposition.

Proposition 3 *Model* (7) *has a trivial equilibrium* $E_{2,0}$ *that is locally asymptotically stable if and only if* $R_{0,2} < 1$. *For* $R_{0,2} \geq 1$, *an endemic equilibrium* $E_{2,1}$ *does exist and is locally asymptotically stable whenever it exists*.

Different values of the model parameters that satisfy the stability condition of the steady state $E_{2,0}$ have been considered. The simulations show that the solutions do not depend on the initial values of $x(0)$ and $y(0)$. Figure 3(a), (b) show tolerance of the immune response,

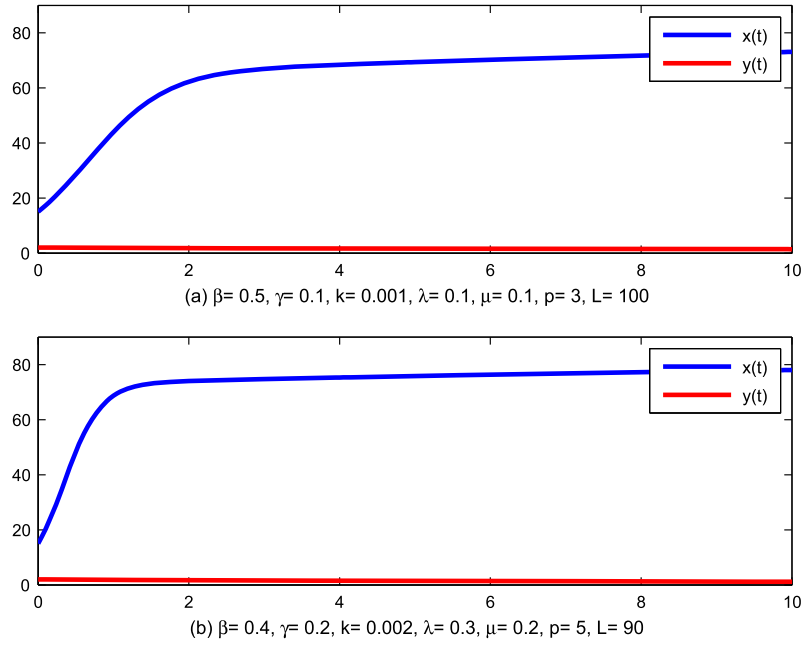

Figure 3 The curves of $x(t)$ and $y(t)$ at different values of the parameters and at the initial point $x(0) = 15$, $y(0) = 2$

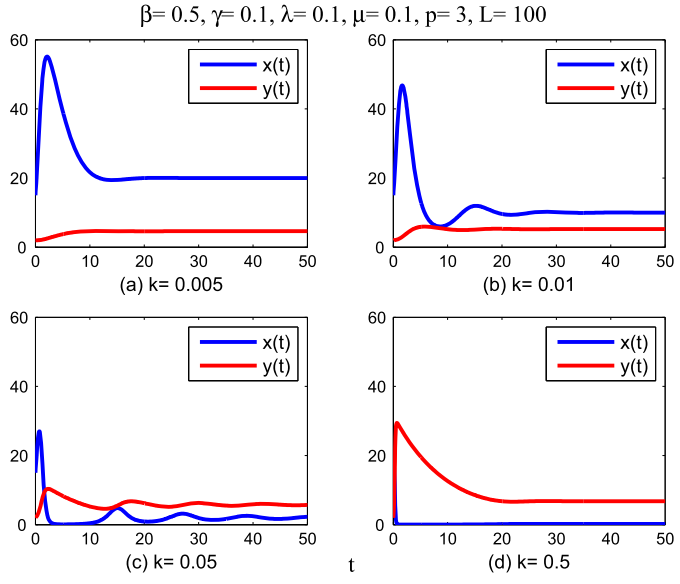

Figure 4 The curves of the target cells $x(t)$ and the induced immune cells $y(t)$ at $\lambda = 0.1$, $\mu = 0.1$, $\beta = 0.5$, $\gamma = 0.1$, $p = 3$, and $L = 100$ and different values of the parameter k

i.e., the induced immune cells cannot be activated, $y(t)$ vanishes, and the autoimmune disease does not develop.

Figure 4 describes different cases of the autoimmune symptoms which depend on the value of the parameter k. Figure 4(a), where $k = 0.005$, shows a scarce evolution of the induced immune cells, but the target cells still predominate the disease, and there are

no symptoms. Figure 4(b), where $k = 0.01$, exhibits a decreasing of the target cells and increase of the induced immune cells, which shows a relatively low level of target cells and mild symptoms. Figure 4(c), where $k = 0.05$, shows repeated flare-up of the autoimmune disease. Figure 4(d), where $k = 0.5$, exhibits rapid progression of the disease and severe symptoms. Note that the target cells suddenly decrease and there is only a few of them in the chronic case. Therefore, the patient with a higher value of k has a higher probability of developing an autoimmune disease. Also, increasing the value of k makes the case of the patient move from tolerance to acute to chronic.

4 Holling type III immune response function

4.1 Linear target cell growth function

Different patients may have different immune response functions. This may be due to the kind of the immune cells or the patient's condition. Here, we propose that the evolution of the target cells population, in the simplest form, is a linear function of $x(t)$, but the evolution of the immune cells is a functional response of Holling type III. Then our model can take the following form:

$$\begin{aligned} \frac{dx(t)}{dt} &= \lambda - \mu x(t) - \beta x(t) y(t), \\ \frac{dy(t)}{dt} &= \frac{m x(t)^2 y(t)^2}{h^2 + x(t)^2 y(t)^2} - \gamma y(t), \end{aligned} \tag{12}$$

where the parameter m is the maximum proliferation rate of immune cells caused by the antigen presented cells (APCs). The parameter h is the number of damaged cells at which the proliferation of immune cells is half of the maximum m. Then the term $mx(t)^2y(t)^2/(h^2 + x(t)^2y(t)^2)$ is the proliferation rate of immune cells by APCs. This nonlinear personal immune response function is biologically more reasonable than the linear one. This model represents cross-reactivity in the immune system. Here, we consider only the case $\mu \geq \gamma$.

4.1.1 Equilibria and stability

To evaluate the steady states $(\overline{x}, \overline{y})$ of system (12), we put

$$\begin{aligned} \left.\frac{dx(t)}{dt}\right|_{(\overline{x},\overline{y})} &= F_1(\overline{x}, \overline{y}) = 0, \\ \left.\frac{dy(t)}{dt}\right|_{(\overline{x},\overline{y})} &= F_2(\overline{x}, \overline{y}) = 0. \end{aligned} \tag{13}$$

On solving the equations of system (13), we get the following three steady states:

$$E_{3,0} = \left(\frac{\lambda}{\mu}, 0\right)', \qquad E_{3,1} = (\overline{x}_-, \overline{y}_-)', \qquad E_{3,2} = (\overline{x}_+, \overline{y}_+)',$$

where

$$\overline{y}_- = \frac{(m\lambda^2 - 2\beta\gamma\mu h^2) - \sqrt{(m\lambda^2 - 2\beta\gamma\mu h^2)^2 - 4\gamma^2 h^2 \mu^2 (\beta^2 h^2 + \lambda^2)}}{2\gamma(\beta^2 h^2 + \lambda^2)},$$

$$\overline{y}_+ = \frac{(m\lambda^2 - 2\beta\gamma\mu h^2) + \sqrt{(m\lambda^2 - 2\beta\gamma\mu h^2)^2 - 4\gamma^2 h^2\mu^2(\beta^2 h^2 + \lambda^2)}}{2\gamma(\beta^2 h^2 + \lambda^2)},$$

and

$$\overline{x}_- = \frac{\lambda}{(\mu + \beta\overline{y}_-)}, \qquad \overline{x}_+ = \frac{\lambda}{(\mu + \beta\overline{y}_+)}.$$

Simple computations show that both equilibria $E_{3,1}$ and $E_{3,2}$ do exist if and only if

$$m \geq \frac{2h\mu\gamma}{\lambda^2}\left(h\beta + \sqrt{\lambda^2 + h^2\beta^2}\right) := m^\star. \tag{14}$$

The following proposition summarizes the above results.

Proposition 4 *In addition to the trivial equilibrium $E_{3,0}$ that exists under no constraint, model (12) has two positive endemic equilibria $E_{3,1}$ and $E_{3,2}$, which exist if and only if the maximum proliferation rate m is greater or equal to the critical level $m^\star$ given by formula (14).*

It is easy to check that

$$\lim_{m\to\infty} \overline{y}_- = 0, \qquad \lim_{m\to\infty} \overline{y}_+ = \infty, \quad \text{and} \quad \overline{y}_-(m^\star) = \overline{y}_+(m^\star). \tag{15}$$

Hence, model (12) does not have a basic reproduction number. Moreover, $m^\star$ is the critical proliferation rate [25, 26] above which endemic equilibria do exist, while below which no endemic equilibrium exists, see Fig. 5. Motivated by the work shown in [24], the ratio $m/m^\star$ is the minimum eradication effort of the disease. Therefore, we show the following proposition.

Proposition 5 *Model (12) has no basic reproduction number, and the minimum effort required to clear the infection is $m\lambda^2/[2h\mu\gamma(h\beta + \sqrt{\lambda^2 + h^2\beta^2})]$.*

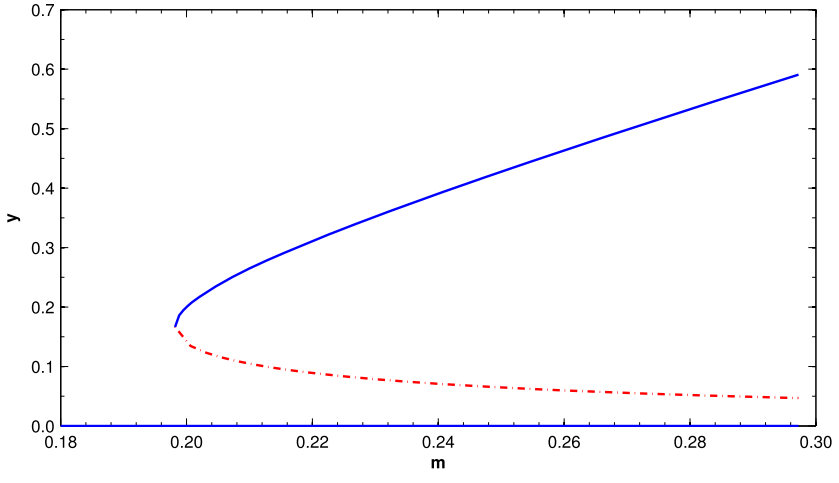

Figure 5 Bifurcation diagram for model (12) with parameter values $\lambda = 10$, $\mu = 0.1$, $\beta = 0.5$, $\gamma = 0.1$, and $h = 30$. The solid curves correspond to the stable equilibria ($\bar{E}_{3,2}$ for the higher line and $\bar{E}_{3,0}$ for the lower line), while the dashed-dotted horizontal line corresponds to the unstable equilibrium $\bar{E}_{3,1}$

To study the local stability of these steady states, we linearize system (12) and compute the Jacobian matrix at each steady state. At the trivial equilibrium $E_{3,0} = (\frac{\lambda}{\mu}, 0)'$, the Jacobian matrix reads

$$J_{3,0} = \begin{pmatrix} -\mu & -\frac{\beta\lambda}{\mu} \\ 0 & -\gamma \end{pmatrix}.$$

It has the eigenvalues $\epsilon_1 = -\mu < 0$, $\epsilon_2 = -\gamma < 0$. Hence, the boundary equilibrium point $E_{3,0}$ is always locally asymptotically stable.

The Jacobian matrix, for model (12), evaluated at the conjugate interior equilibria $E_{3,1} = (\overline{x}_-, \overline{y}_-)'$ and $E_{3,2} = (\overline{x}_+, \overline{y}_+)'$ is

$$J_{3,1} = \begin{pmatrix} -\frac{\lambda}{\overline{x}_-} & -\beta\overline{x}_- \\ \frac{2\gamma^2h^2}{m\overline{x}_-^3} & \frac{2\gamma^2h^2}{m\overline{x}_-^2\overline{y}_-} - \gamma \end{pmatrix} \quad \text{and} \quad J_{3,2} = \begin{pmatrix} -\frac{\lambda}{\overline{x}_+} & -\beta\overline{x}_+ \\ \frac{2\gamma^2h^2}{m\overline{x}_+^3} & \frac{2\gamma^2h^2}{m\overline{x}_+^2\overline{y}_+} - \gamma \end{pmatrix},$$

respectively. It is clear that the trace of the Jacobian matrix at the endemic equilibrium $(\bar{x}, \bar{y})'$ is

$$\begin{aligned} \operatorname{tr}(J) &= \frac{2\gamma^2h^2}{m\bar{x}^2\bar{y}} - \frac{\lambda}{\bar{x}} - \gamma \\ &= \frac{2\gamma^2h^2}{m\lambda^2\bar{y}}(\mu + \beta\bar{y})^2 - (\mu + \beta\bar{y}) - \gamma \\ &= \frac{1}{m\lambda^2\bar{y}}\big[\big(2\mu\gamma^2h^2 + \big(2\beta\gamma^2h^2 - m\lambda^2\big)\bar{y}\big)(\mu + \beta\bar{y}) - m\gamma\lambda^2\bar{y}\big] \\ &= \frac{1}{m\lambda^2\bar{y}}\big[\beta\big(2\beta\gamma^2h^2 - m\lambda^2\big)\bar{y}^2 + \big(4\mu\beta\gamma^2h^2 - m\lambda^2(\mu + \gamma)\big)\bar{y} + 2\gamma^2h^2\mu^2\big] \\ &= \frac{-1}{m}\big[\big(\beta m + 2\gamma^2\big)\bar{y} + m(\mu - \gamma)\big] < 0. \end{aligned}$$

However, the determinant of the Jacobian matrix evaluated at any endemic equilibrium $(\bar{x}, \bar{y})'$ is

$$\begin{aligned} \det(J) &= \frac{\lambda}{\bar{x}}\left(\gamma - \frac{2\gamma^2h^2}{m\bar{x}^2\bar{y}}\right) + \frac{2\beta\gamma^2h^2}{m\bar{x}^2} = \frac{1}{\bar{x}}\left(\gamma\lambda - \frac{2\gamma^2h^2\lambda}{m\bar{x}^2\bar{y}} + \frac{2\beta\gamma^2h^2}{m\bar{x}}\right) \\ &= \frac{\gamma}{\bar{x}}\left(\lambda - \frac{2\gamma\mu h^2}{m\lambda}\left(\beta + \frac{\mu}{\bar{y}}\right)\right) = \frac{\gamma}{m\lambda\bar{x}\bar{y}}\big(\big(m\lambda^2 - 2\gamma\mu\beta h^2\big)\bar{y} - 2\gamma\mu^2h^2\big) \\ &= \frac{\gamma}{m\lambda\bar{x}}\big(2\mu\beta\gamma h^2 - m\lambda^2 + 2\gamma\big(\lambda^2 + \beta^2h^2\big)\bar{y}\big). \end{aligned}$$

Hence, for the equilibrium $E_{3,1}$, the determinant of its corresponding Jacobian is

$$\det(J_{3,1}) = \frac{-\gamma}{m\lambda\bar{x_-}}\sqrt{\big(m\lambda^2 - 2\beta\gamma\mu h^2\big)^2 - 4\gamma^2h^2\mu^2\big(\beta^2h^2 + \lambda^2\big)} < 0.$$

However, for the equilibrium $E_{3,2}$, the determinant of its corresponding Jacobian is

$$\det(J_{3,2}) = \frac{\gamma}{m\lambda\bar{x_+}}\sqrt{\big(m\lambda^2 - 2\beta\gamma\mu h^2\big)^2 - 4\gamma^2h^2\mu^2\big(\beta^2h^2 + \lambda^2\big)} > 0.$$

Thus, the endemic equilibrium $E_{3,1}$ is unstable whenever it exists, while the endemic equilibrium $E_{3,2}$ is locally asymptotically stable whenever it exists, and we show the following proposition.

Proposition 6 *Model* (12) *has a trivial equilibrium* $E_{3,0}$ *that always exists and is always locally asymptotically stable. If* $m \geq m^{\star}$, *two endemic equilibria* $E_{3,1}$ *and* $E_{3,2}$ *start to appear, where* $E_{3,1}$ *is always unstable, while* $E_{3,2}$ *is always locally asymptotically stable.*

4.1.2 Transient behavior

In order to see the dynamics of the components x and y, the local and global attractors of the model, and to appropriately present our results, we project the first quadrant $\{(x,y) : 0 \leq x, y < \infty\}$ on the square $\{(X,Y) : 0 < X, Y \leq 1\}$ using the transformation

$$X = \frac{1}{1+x} \quad \text{and} \quad Y = \frac{1}{1+y}. \tag{16}$$

Hence, model (12) could be rewritten as

$$\begin{aligned} \frac{dX}{dt} &= -X^2\left[\lambda + \mu - \frac{\mu}{X} - \beta\left(\frac{1}{X} - 1\right)\left(\frac{1}{Y} - 1\right)\right], \\ \frac{dY}{dt} &= -Y^2\left[\frac{m(1-X)^2(1-Y)^2}{h^2X^2Y^2 + (1-X)^2(1-Y)^2} - \gamma\left(\frac{1}{Y} - 1\right)\right]. \end{aligned} \tag{17}$$

Model (17) has the three equilibria

$$\bar{E}_{1,0} = \left(\frac{\mu}{\lambda+\mu}, 1\right)', \qquad \bar{E}_{3,1} = (X_{3,1}, Y_{3,1})', \quad \text{and} \quad \bar{E}_{1,1} = (X_{3,2}, Y_{3,2})', \tag{18}$$

which correspond, respectively, to $E_{3,0}$, $E_{3,1}$, and $E_{3,2}$, where

$$X_{3,1} = \frac{\mu + \beta\bar{y}_-}{\lambda + \mu + \bar{y}_-}, \qquad X_{3,2} = \frac{\mu + \beta\bar{y}_+}{\lambda + \mu + \bar{y}_+}, \qquad Y_{3,1} = \frac{1}{1+\bar{y}_-}, \quad \text{and} \quad Y_{3,2} = \frac{1}{1+\bar{y}_+}.$$

Figure 6 shows the trajectory analysis of the model. Part (a) is produced with parameter values corresponding to $m < m^{\star}$, where no endemic equilibrium exists. Thus, the trivial equilibrium $\bar{E}_{3,0}$ is the global attractor. However, part (b) is drawn with parameter values as shown in the legend of Fig. 6 and a value of $m > m^{\star}$, where two endemic equilibria coexist with the trivial one. It shows that $\bar{E}_{3,0}$ and $\bar{E}_{3,2}$ are the only two attractors for the trajectories, while $\bar{E}_{3,1}$ lies on the separating between the basin of attractors for $\bar{E}_{3,0}$ and $\bar{E}_{3,2}$.

Based on the strategy shown in [24], it is noteworthy that the disease could be cleared if control measures aiming at reducing the rate m to slightly less than $m^{\star}$ have been applied. Moreover, for $m \geq m^{\star}$, solutions depend on the initial conditions [27] in the sense that the fate of a trajectory (i.e., the attractor) could either be the trivial equilibrium $E_{3,0}$ or the stable endemic equilibrium $E_{3,2}$ depending on the initial conditions, see Fig. 6. If we consider the bifurcation diagram (see Fig. 5) in the plane $(m, \bar{y})$, then the level of $\bar{y}$ corresponding to the unstable equilibrium $E_{3,1}$ is sometimes called the break point. Numerical

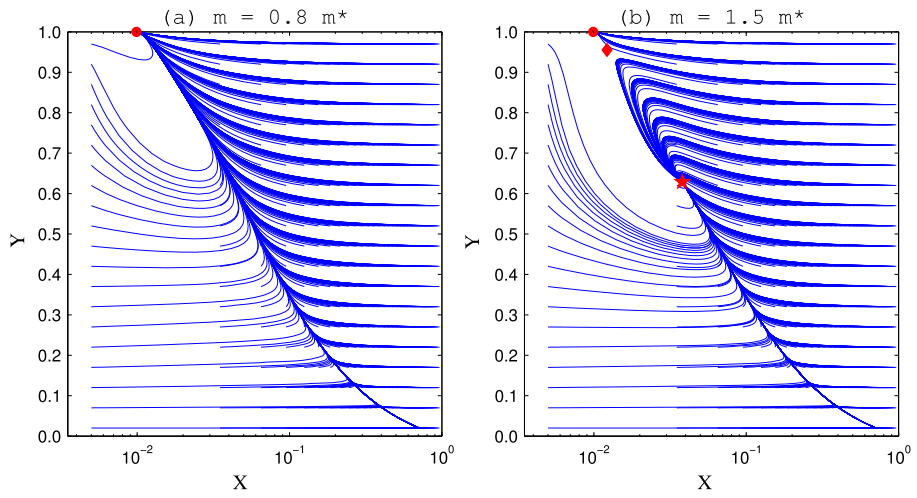

Figure 6 The trivial equilibrium $\bar{E}_{3,0}$ is represented by the circle "•", the unstable endemic equilibrium $\bar{E}_{3,1}$ is denoted by the rhombus "♦", and the stable endemic equilibrium $\bar{E}_{3,2}$ is represented by the star "★". Simulations have been done with parameter values $\lambda = 10$, $\mu = 0.1$, $\beta = 0.5$, $\gamma = 0.1$, and $h = 30$. Part (**a**) is produced with $m = 0.8m^{\star}$, while part (**b**) is produced with $m = 1.5m^{\star}$

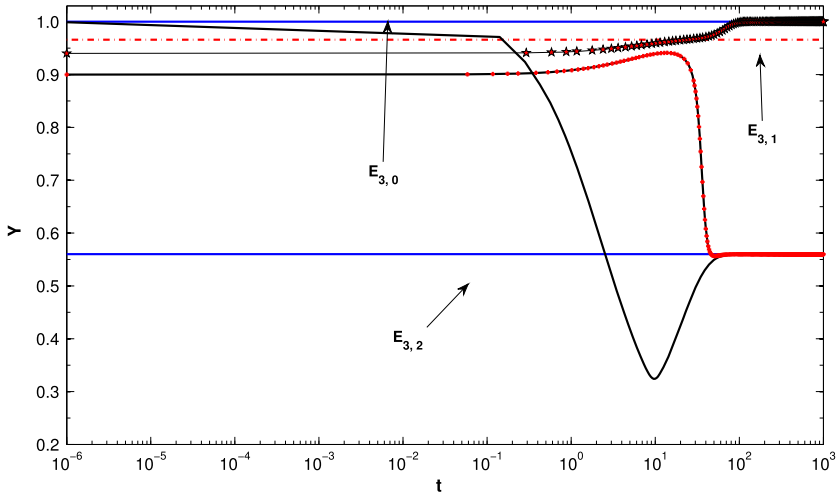

Figure 7 Time-series analysis for model (17) with parameter values $\lambda = 10$, $\mu = 0.1$, $\beta = 0.5$, $\gamma = 0.1$, $h = 30$, and $m = 1.8m^{\star}$. The solid horizontal lines correspond to the stable equilibria ($\bar{E}_{3,0}$ for the higher line and $\bar{E}_{3,2}$ for the lower line), while the dashed-dotted horizontal line corresponds to the unstable equilibrium $\bar{E}_{3,1}$. The trajectory of solid curve signed with stars "★" is produced with initial values $X = 0.03$ and $Y = 0.94$, while that signed with pluses "+" has initial data $X = 0.0001$ and $Y = 0.999$. The sign-free solid trajectory curve is produced with initial conditions $X = 0.1$ and $Y = 0.9$

simulations show that even if y is reduced to below the break point, it is not necessary that the trajectory is attracted by the trivial equilibrium, see Fig. 7.

4.2 Nonlinear target cell growth function

In this subsection, we propose that the evolution of the target cells population is a nonlinear function of $x(t)$, the logistic form, but the evolution of the immune cells is a functional

response of Holling type III. Then our model can take the following form:

$$\begin{aligned} \frac{dx(t)}{dt} &= \lambda - \mu x(t) + px(t)\left(1 - \frac{x(t)}{L}\right) - \beta x(t)y(t), \\ \frac{dy(t)}{dt} &= \frac{mx(t)^2y(t)^2}{h^2 + x(t)^2y(t)^2} - \gamma y(t). \end{aligned} \tag{19}$$

Here, we consider only the case $\mu \geq \gamma$. To compute the equilibria of this model, we put the derivative in its left-hand side equal to zero and solve the resulting nonlinear algebraic equation in terms of $\overline{x}$ and $\overline{y}$. The analysis shows that it has a trivial equilibrium

$$E_{4,0} = (\overline{\overline{x}}, 0)',$$

where

$$\overline{\overline{x}} = \frac{L}{2p}\left((p-\mu) + \sqrt{(p-\mu)^2 + 4p\lambda/L}\right),$$

under the existence condition $p > \mu$. Moreover, it has other nontrivial (endemic) equilibria

$$E = (\overline{x}, \overline{y})',$$

whose components $\overline{x}$ and $\overline{y}$ are defined through

$$F(\bar{x}) = a_0\overline{x}^4 + a_1\overline{x}^3 + a_2\overline{x}^2 + a_3\overline{x} + a_4 = 0, \tag{20}$$

$$\overline{y} = \frac{\lambda}{\beta\overline{x}} + \frac{(p-\mu)}{\beta} - \frac{p\overline{x}}{\beta L}, \tag{21}$$

where

- $a_0 = \gamma p^2 > 0$,
- $a_1 = Lp(\beta m - 2\gamma(p-\mu))$,
- $a_2 = L(\gamma(p-\mu)^2 L - m\beta(p-\mu)L - 2\gamma\lambda p)$,
- $a_3 = \lambda L^2(2\gamma(p-\mu) - m\beta)$,
- $a_4 = \gamma L^2(h^2\beta^2 + \lambda^2) > 0$.

Once a solution $\bar{x}$ for (20) is obtained, we substitute in (21) to get its corresponding $\bar{y}$. However, $\bar{x}$ is the root of a fourth degree polynomial. Before studying the existence of feasible solutions for (20), we state the following theorem that is known as "Descartes' rule of signs" and determines the number of positive and negative real roots for any polynomial.

Theorem 7 (Descartes' rule of signs [28]) *Let $F(x)$, written in ascending or descending order, be a polynomial function with constant real coefficients and have nonzero constant term. Then*:

The number of positive real zeros of $F(x)$ is either:

1. *The same as the number of variations of the sign in $F(x)$, or*
2. *Less than the number of variations of the sign in $F(x)$ by a positive even integer.*

The number of negative real zeros of $P(x)$ is either:

1. *The same as the number of variations of the sign in $F(-x)$, or*

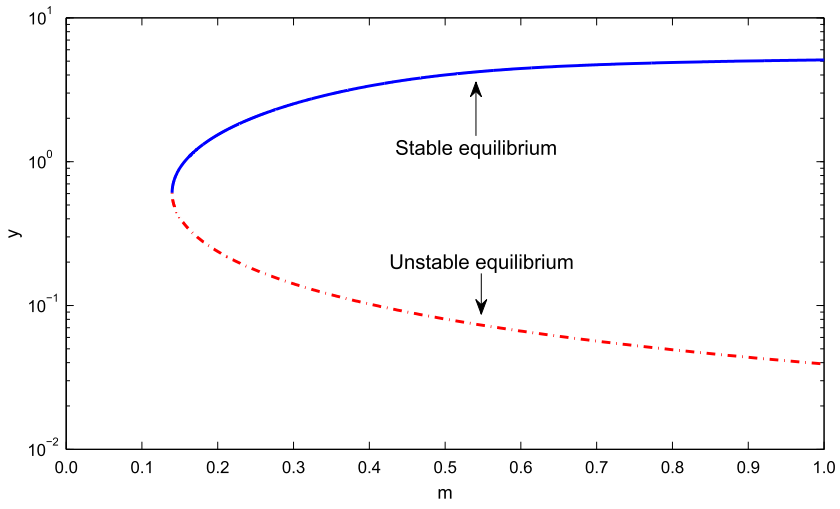

Figure 8 Bifurcation diagram in the plane $(m,\bar{y})$ for parameter values $\lambda = 0.1$, $\mu = 0.1$, $\beta = 0.5$, $\gamma = 0.1$, $h = 60$, $p = 3$, and $L = 100$. The diagram shows that two endemic equilibria do exist for high enough values of m. The dashed-dotted curve corresponds to the unstable endemic equilibrium, while the solid one corresponds to the stable endemic equilibrium

2. *Less than the number of variations of the sign in $F(-x)$ by a positive even integer. A zero of multiplicity N must be counted N times.*

We are concerned only with the positive real roots of this fourth degree equation (20). Taking into account that both a_0 and a_4 are positive, while a_1 and a_3 have different signs, depending on the value of m with respect to the other parameters, then, regardless of the sign of a_2, equation (20) will have either two positive real roots (say, $\bar{x}_1$ and $\bar{x}_2$) or it will have no root. Except m, if all other parameters have been kept fixed, then high enough values of m ensure the existence of two feasible (positive) solutions for (20), while small enough values of m show non-existence of positive solutions for (20), see Fig. 8. Consequently, we compute the corresponding values of y at equilibrium, and therefore model (19) will have either two conjugate interior equilibria or no interior equilibrium. When it exists, the interior equilibrium corresponding to the higher feasible solution of $\bar{y}$ is expected to be locally asymptotically stable, while its conjugate is unstable.

A bifurcation diagram in the plane (λ, m) is shown in Fig. 9. The diagram shows the critical value of m (say, $m^{\star}$) separating between non-existence and existence of positive endemic equilibria. If the pair (λ, m) is chosen below this curve, then model (19) will have only the trivial equilibrium $E_{4,0}$, while if this pair is chosen from the region above that curve, then model (19) will have two endemic equilibria, in addition to the trivial equilibrium $E_{4,0}$.

Similar to the case of model (12), the current model has no basic reproduction number and, for some range of the parameters, the model exhibits multiple endemic equilibria. Thus, clearing the disease depends on the initial conditions, or could be implemented by applying control measures aiming to reduce m to slightly below the threshold $m^{\star}$.

Following the same way as in section (4.1.2) and using transformation (16), the current model is simulated. Figure 10 confirms our analytical results, where the model has two

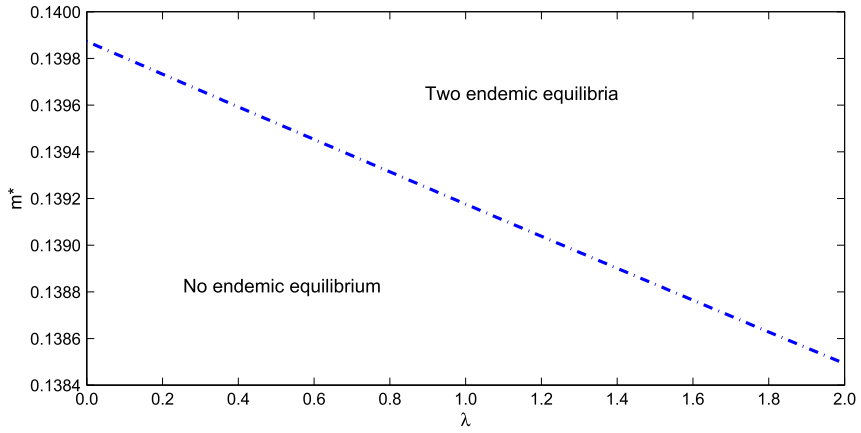

Figure 9 Bifurcation diagram in the plane (λ, m^*) for parameter values $\mu = 0.1$, $\beta = 0.5$, $\gamma = 0.1$, $h = 60$, $p = 3$, and $L = 100$. The curve shows the critical value of m below which no endemic equilibrium exists, while above which two endemic equilibria do exist

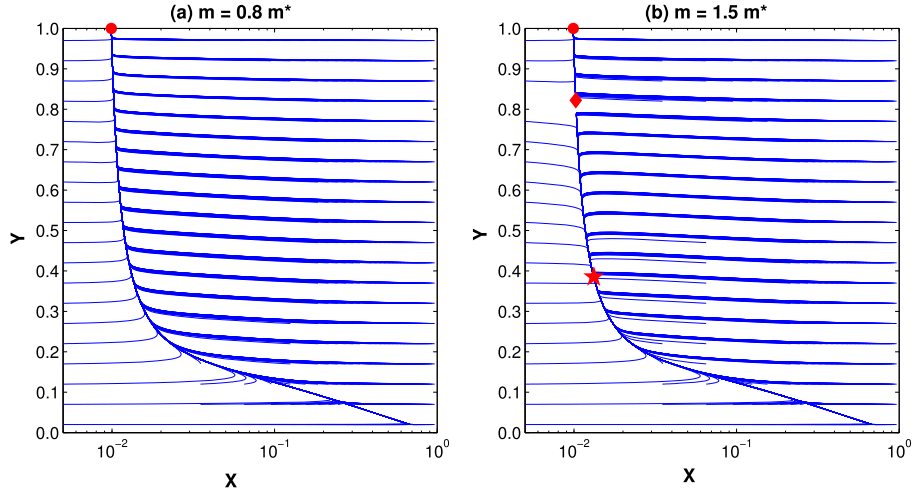

Figure 10 The trivial equilibrium $\bar{E}_{4,0}$ is represented by the circle "●", the unstable endemic equilibrium $\bar{E}_{4,1}$ is denoted by the rhombus "♦" and the stable endemic equilibrium $\bar{E}_{4,2}$ is represented by the star "★". Simulations have been done with parameter values $\lambda = 10$, $\mu = 0.1$, $\beta = 0.5$, $\gamma = 0.1$, $h = 60$, $p = 3$, and $L = 100$. Part (**a**) is produced with $m = 0.8m^\star$, while part (**b**) is produced with $m = 1.5m^\star$, where $m^\star = 0.1335$

endemic equilibria for high enough values of m (i.e., $m > m^\star$), while it has no endemic equilibrium if $m < m^\star$.

5 Summary and conclusion

Guillain–Barré syndrome (GBS) is potentially life threatening. GBS patients are supposed to be admitted for monitoring. They have to monitor breathing, heart rate, and blood pressure. When a patient's ability to breathe is impaired, they have to be put on a ventilator. All patients have to be observed for such complications as infection, changes of blood pressure, blood coagulating changes, or heart beat changes. GBS has unknown cure, while treatment improves symptoms and decreases duration. Given the autoimmune nature of the disease, its acute phase is typically treated with immunotherapy such as plasma ex-

change to remove antibodies from the blood or intravenous immunoglobulin. It is considered as autoimmune disease, so treatment is either plasma exchange to decrease blood antibodies or intravenous immunoglobulin. It is effective if used 7 to 10 days from the beginning of symptoms. If muscle weakness persists after acute phase treatment, the patient will be treated by rehabilitation.

To the best of our knowledge this is the first mathematical model for GBS. The interaction between the target cells and the immune cell inducement is generally described by model (1). Depending on the form of the target cell growth and the immune response, four cases of the model have been studied. In cases where the immune response is assumed to be linear, the model has a basic reproduction number (BRN) which is a function of the activation rate of the immune response k. If the BRN is reduced to below one (i.e., k reduces to below some threshold), then the disease dies out where the trivial equilibrium is globally stable, while if the BRN is higher than one (i.e., k is above this threshold), then a unique endemic equilibrium exists and is locally asymptotically stable, which means that the disease persists. In the cases where the immune response is assumed to be nonlinear and in the form of Holling type III, the model does not have a basic reproduction number. Moreover, the model has a trivial equilibrium that is always locally asymptotically stable. However, if all parameters have been kept fixed except the maximum proliferation rate of the immune cells m, then, for m above some threshold (denoted by $m^\star$), two conjugate endemic equilibria start to appear. The endemic equilibrium with higher level of immune cell inducement y^+ is always locally stable, while the other is unstable. This behavior means that the initial conditions play a role in the fate of trajectories. In other words, clearing the disease depends on the initial conditions. Motivated by the work shown in [24], our results show that control measures aiming at reducing the maximum proliferation rate m to slightly below the critical threshold $m^\star$ ensure a successful elimination of the disease. Our results show further that early detection of the disease gives a better chance of cure since the value of y_0 is small enough.

Acknowledgements
The authors would like to thank the editor as well as the anonymous referees very much for their invaluable comments which helped in improving the paper.

Funding
The authors extend their appreciation to the Deanship of Scientific Research at King Khalid University for funding this work through Big Group Research Project under grant number (G.R.P2/16/40).

Competing interests
The authors declare that they have no competing interests.

Authors' contributions
The authors contributed equally and significantly in writing this paper. All authors read and approved the final manuscript.

Author details
[1]Mathematics Department, Faculty of Science, King Khalid University, Abha, Saudi Arabia. [2]Mathematics Department, Faculty of Science, Mansoura University, Mansoura, Egypt. [3]Department of Mathematical Sciences, Faculty of Applied Science, Umm Al-Qura University, Makkah, Saudi Arabia.

Received: 15 December 2018 Accepted: 20 May 2019 Published online: 29 May 2019

References

1. Horwitz, M.S., Sarvetnick, N.: Viruses, host responses, and autoimmunity. Immunol. Rev. **169**, 241–253 (1999)
2. von Herrath, M.G., Oldstone, M.B.: Viruses-induced autoimmune diseases. Curr. Opin. Immunol. **8**, 878–885 (1996)
3. Iwami, S., Takeuchi, Y., Miura, Y., Sasaki, T., Kajiwara, T.: Dynamical properties of autoimmune disease models: tolerance, flare-up, dormancy. J. Theor. Biol. **246**, 646–659 (2007)
4. Sejvar, J.J., Baughman, A.L., Wise, M., Morgan, O.W.: Population incidence of Guillain–Barré syndrome: a systematic review and meta-analysis. Neuroepidemiology **36**, 123–133 (2011)
5. ven den Berg, B., Walgaard, C., Drenthen, J., Fokke, C., Jacobs, B.C., van Doorn, P.A.: Guillain–Barré syndrome: pathogenesis, diagnosis, treatment and prognosis. Nat. Rev. Neurol. **10**, 469–482 (2014)
6. Darweesh, S.K., Polinder, S., Mulder, M.J., Baena, C.P., van Leeuwen, N., Franco, O.H., Jacobs, B.C., van Doorn, P.A.: Health-related quality of life in Guillain–Barré syndrome patients: a systematic review. J. Peripher. Nerv. Syst. **19**, 24–35 (2014)
7. Guillain–Barré syndrome. https://www.who.int/en/news-room/fact-sheets/detail/guillain-barr
8. Hughes, R., Wijdicks, E., Barohn, R., Benson, E., Cornblath, D., Hahn, F., Meythaler, J., Miller, R., Sladky, J., Stevens, J.: Practice parameter: immunotherapy for Guillain-Barré syndrome: report of the Quality Standards Subcommittee of the American Academy of Neurology. Neurology **61**(6), 736–740 (2003)
9. Dantal, J.: Intravenous immunoglobulins: in-depth review of excipients and acute kidney injury risk. Am. J. Nephrol. **38**(4), 275–284 (2013)
10. Dimachkie, M., Barohn, R.: Guillain–Barré syndrome and variants. Neurol. Clin. **31**(2), 491–510 (2013)
11. Uncini, A., Kuwabara, S.: Electrodiagnostic criteria for Guillain–Barré syndrome: a critical revision and the need for an update. Clin. Neurophysiol. **123**(8), 1487–1495 (2012)
12. Wakerley, B., Uncini, A., Yuki, N.: Guillain–Barré and Miller Fisher syndromes—new diagnostic classification. Nat. Rev. Neurol. **10**(9), 537–544 (2014)
13. Uncini, A., Shahrizaila, N., Kuwabara, S.: Zika virus infection and Guillain–Barré syndrome: a review focused on clinical and electrophysiological subtypes. J. Neurol. Neurosurg. Psychiatry **88**(3), 266–271 (2016)
14. Bonyah, E., Khan, M.A., Okosun, K.O., Islam, S.: A theoretical model for Zika virus transmission. PLoS ONE **12**(10), e0185540 (2017)
15. Bonyah, E., Okosun, K.O.: Mathematical modeling of Zika virus. Asian Pac. J. Trop. Dis. **6**(9), 673–679 (2016)
16. Baca-Carrasco, D., Velasco-Hernández, J.X.: Sex, mosquitoes and epidemics: an evaluation of Zika disease dynamics. Bull. Math. Biol. **78**, 2228–2242 (2016)
17. Andayani, P., Sari, L.R., Suryanto, A., Darti, I.: Numerical study for ZIKA virus transmission with Beddington–Deangelis incidence rate. Far East J. Math. Sci. **111**(1), 145–157 (2019)
18. Moya, E.M.D.: Mathematical model for the ZIKA epidemic using ordinary equations and with temporary delay. Proc. Ser. Braz. Soc. Comput. Appl. Math. **6**(2) (2018). https://doi.org/10.5540/03.2018.006.02.0289
19. Charles, W.M., George, L.O., Malinzi, J.: A spatiotemporal model on the transmission dynamics of Zika virus disease. Asian Res. J. Math. **10**(4), 1–15 (2018)
20. Nowak, M.A., Bangham, C.R.M.: Population dynamics of immune responses to persistent viruses. Science **272**, 74–79 (1996)
21. Nowak, M.A., May, R.M.: Virus Dynamics. Oxford University Press, Oxford (2000)
22. Perelson, A.S., Nelson, P.W.: Mathematical analysis of HIV-1 dynamics in vivo. SIAM Rev. **41**, 3–44 (1998)
23. De Leenheer, P., Smith, H.L.: Virus dynamics: a global analysis. SIAM J. Appl. Math. **63**, 1313–1327 (2003)
24. Safan, M., Heesterbeek, H., Dietz, K.: The minimum effort required to eradicate infections in models with backward bifurcation. J. Math. Biol. **53**, 703–718 (2006)
25. Safan, M., Dietz, K.: On the eradicability of infections with partially protective vaccination in models with backward bifurcation. Math. Biosci. Eng. **6**(2), 395–407 (2009)
26. Safan, M., Kretzschmar, M., Hadeler, K.: Vaccination based control of infections in SIRS models with reinfection: special reference to pertussis. J. Math. Biol. **67**, 1083–1110 (2013)
27. Safan, M., Rihan, F.A.: Mathematical analysis of an SIS model with imperfect vaccination and backward bifurcation. Math. Comput. Simul. **96**, 195–206 (2014)
28. Bittinger, M.L., Beccher, J.A., Ellenbogen, D.J., Penna, J.A.: Precalculus, Graphs, and Models: A Right Triangle Approach, 5th edn. Pearson Education, Upper Saddle River (2013)